Effects of Tube Arrangement on Flow Distribution in the Header of Shell and Tube Heat Exchangers

Zakarya Madaoui [1,*], Omar Labbadlia[2], Mohamed Abbadeni[3], Younes Chiba[2], Mounir Zirari[2].

[1] Faculty of technology, mechanical engineering department, university of Fares Yahya, medea, 26000, Algeria.

[2] Renewable energy and materials laboratory, LERM, university of Fares Yahya, medea, 26000, Algeria.

[3]Faculty of Science and Technology, University of DjilaliBounaama, Khemis Miliana, 44225, Algeria.

(Corresponding Author):*E-mail: zkrmadaoui@yahoo.fr

Received: 09-04-2023 **Accepted:** 24-07-2023 **Published:** 26-07-2023

Abstract*:* The behavior of the fluid inside the internal circulation system of shell and tube heat exchanger is complex and there is a high number of influencing factors. The flow distribution is an important matter, because it has a significant influence on the performance of fluidic devices such as tubular heat exchangers. Non-uniformity of the flow distribution reduces the efficiency of the process, because some of the components become inefficient. In this paper, the influence of tubes arrangements on the flow distribution have been studied through numerical simulations. The results showed that arrangement of the tubes has an influence on the distribution of the flow. The arrangements of 45° and 60°, respectively, provide the flow with a good velocity distribution at a maximum number of tubes compared to the other arrangements. The results obtained are in good agreement with the existing results from the literature.

Key words: Simulation, Heat exchangers, Fluids, Flow distribution, Velocity.

Tob Regul Sci.™ 2023;9(1): 3700-3711
DOI: doi.org/10.18001/TRS.9.1.259

1. Introduction

Heat exchangers are devices that allow the transfer of heat energy between two fluids, and are somewhat crucial in many processes. They are widely used in the chemical, pharmaceutical and petrochemical industries, in power plants and many other applications. There are several types of heat exchangers, such that choosing the right one for a particular process is not a simple procedure. In fact, it is known that choosing the wrong type for a particular plant can lead to suboptimal performance, operational problems and equipment failure. One frequently used type is the tubular heat exchanger, which has the advantage of rapidly offering a large heat transfer surface and is compact. Design: The basic design aspect of this type of exchanger is to try to make the flow distribution as uniform as possible [1, 2] In fact, irregularity is one of the main reasons that are known to significantly reduce the performance of heat exchangers [1, 2].

Limited work has been done in the field of flow distribution within the split inlet manifold of a tubular heat exchanger. Venkatesan [2] conducted a non-numerical study related to the maldistribution of heat exchanger flow and heat exchanger. The flow field in the exchanger head was obtained by solving the mass and momentum conservation equations using the k-turbulence model, in addition, the authors used two heads with variable lengths, and the obtained results indicated that the regularity of the flow

distribution is inversely proportional to the length of the head. As such, the length of the head will result in a more irregular flow distribution. What's more, the static pressure will be nearly equal for all tubes in the conical head case. Akrivosites et al. [3] predicted that downstream conditions do not influence the determination of lateral flow in the stream pipes, and also indicated that a wider cross-sectional area in the collectors would improve the flow distribution further. Kubo and Ueda [4] found that the quality of the flow distribution is independent of the range of the Reynolds number between 30,000 and 100,000, and that the flow distribution will improve if the branch pipe resistance is increased. They also found that the irregularity depends on the computed pressure due to: frictional pressure drops, pressure, flow recovery, and fluid escape from the holes. They reported that a better flow distribution would be obtained if a larger cross-sectional area was used [3, 4]. They recommended placing an overlying perforated plate in order to reduce poor flow distribution, Kobo and Ueda [4]. Mohanet al. [5] found that the flow distribution is a function of the number of tubes, flow volume, and tube size. Sabret Al [6] indicated that the increase in total pressure loss is due to the increase in the kinetic energy of the fluid. Reprovit et al. [7] demonstrated that the third numerical model will correctly predict the flux distribution, while studies by another Gandhi [8] showed that uniformity of the distribution works in both multiple and kinetic input geometries. Moreover, they also found that the configuration that provides a non-uniform distribution is one in which the tubes are aligned with the inlet-outlet port. They also indicated the following: The uniform distribution of the outgoing current was obtained by reducing the diameter of the tube. The reasons behind the phenomenon of largely irregular flow distribution are: pipe diameters, flow velocity; In addition to the decreases in the tubing and the diameter of the inlet manifold. At a constant value of the Reynolds number, the working fluid (air/water) has a nominal effect on the regularity of the phenon for the configurations considered in this work. The flow in split collectors was formulated by a standard equation by the work of Wangit Al. They also found that the distribution of flow and pressure drop in the collectors is controlled by three "general properties" parameters: 1) E: the ratio of the collector's length to diameter (L/D); 2) M: the ratio of the sum of the outlet areas to the head area; 3) ζ: average coefficient of total pressure drop throughput of the port. Lu and colleagues [12] have developed a separate model to account for the flow distribution in the collectors. An experimental evaluation of the parameters of the flow characteristics was performed to support the discrete model. The satisfactory agreement between the empirical and theoretical pressure distributions confirms the validity of the estimated theoretical model and the limitations of the theoretical continuum model. bit al. [13] focused on applications of computational fluid dynamics (CFD) in the field of heat exchangers. They found that CFD has been used in various fields of study such as fluid flow misdistribution, fouling, pressure drops, and thermal analysis in the design and optimization stage, in different types of heat exchangers. These simulations generated largely accurate solutions, demonstrating that CFD is a very effective tool for predicting the behavior and performance of a variety of heat exchangers [1, 13, 14] Rohsinoff and Putnam [15] found that erratic distribution and unstable dips are more likely to occur in laminar flow than in turbulent flow. The flow is measured by relating it to the total pressure drop through the pipe bank and the fluid dynamic energy at the header inlet:

$$\frac{\text{maximum velocitythrough a tube}}{\text{averagevelocitythrough the tubes}} = \sqrt{\frac{\Delta P_t + (\frac{1}{2}\rho U^2)_{inlet}}{\Delta P_t}} (1)$$

Where 〖ΔP〗 _ is the total pressure difference, U is the fluid density, U is the velocity.

This equation shows that the flow distribution can be improved by increasing the general pressure drop ΔP〗 until it becomes larger compared to the input velocity term (1/2ρU^2) or by decreasing the term 1/2ρU^2 by the appropriate head size [16, 17]. Types of heat exchangers - large due to the geometric characteristics of the heat exchanger. They report that flow misdistribution is a function of the number of tubes, that is, until the number of tubes increases, the uniform distribution or maximum number of tubes with velocity deviation less than | 5% | It was reported by Kuppan [18] that the use of a small mill may lead to greater heat transfer in this insect and its compaction. However, using the large handle will provide a greater reduction in pressure drop and fouling as well. It has also been noted that the minimum ratio of pitch to outer diameter of the tube is 1.25, as the drawstring may become too low for winding tubes in the tube plate (end plate), and this study clearly showed that the misalignment is not a function of the Reynolds number, but one has to consider the effect of the geometrical aspects of the shell and tube heat exchanger. By analyzing all cited bibliographic references, the majority of researchers agreed that geometric parameters influence flow distribution.

As such, in this paper the particular aspect of the effect of tube arrangement on flow distribution has been studied, using CFD tools. The objective of this paper is to find the best possible arrangement of the tube that can result in a uniform flow distribution.

In this paper, the special aspect of the effect of tube arrangement on flow distribution is investigated, using CFD tools. The goal is to find the best possible arrangement of the tube that can result in a uniform flow distribution. The model of Mohammadi and Malayri [17] is used as a basis for comparison. The numerical approach, which deals with such a configuration, is introduced followed by the details of the numerical method. The simulation results showed that the arrangement of the pipe has a remarkable effect on the flow distribution.

2. Modeling and simulation

We have used CFD instruments to simulate the flow in the atrial heat exchanger head in order to investigate the influence of the internal arrangement on the fluid distribution (Fig. 1a and Fig. 1b). We note that when we talk about the degree of order, it is compared to the flows through the interior of the cortex (Fig. 1c). Four conventional arrangements were performed as shown in Figure 2.

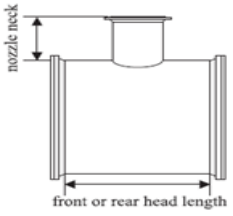

(a)

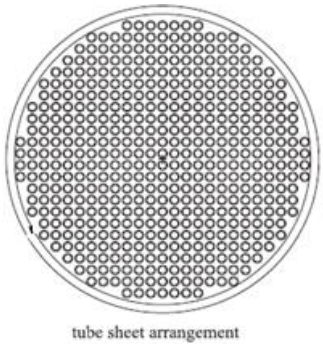

(b)

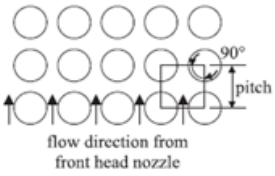

(c)

Fig.1. Typical geometric configuration of medium industrial tubular heat exchanger[17]

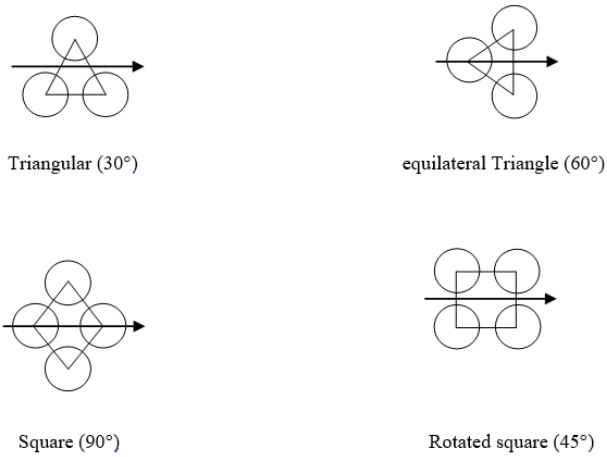

Fig.2. The different tube arrangements to achieve

2.1 Physical model

The selected exchanger is medium industrial type (Fig. 1), and it has one pass with 464 and 461 tubes for two states of arrangement 90° and 45° respectively, 517 and 465 tubes 30° and 60° respectively (Fig. 2). The exchanger parameter values are shown in Table 1.

Table 1: Geometric characteristics of the exchanger

Designation	Value
Diameter of the head (mm)	838.20
Length of the head (mm)	628.65
Neck Length (mm)	377
Diameter of the neck (mm)	387
Tube Diameter (mm)	25.40
Pitch (mm)	31.75
Number of tube for 90°/60°/45°/30°	464/465/461/517

2.2 Governing equations

The equations used in this simulation are the continuity expressed by equation (2), the momentum given by equation (3), and the flow is considered to be the best.

$$\nabla.(\rho\vec{v}) = 0 \quad (2)$$

whereυ is the dynamic viscosity

$$\nabla.(\rho\vec{v}\vec{v}) = -\nabla P + \nabla.(\bar{\bar{\tau}}) + \rho\vec{g} \quad (3)$$

where$\tau$is the shear stress, $g$is the gravitational body force

2.3 Mesh generation

Computing domains are intertwined with an unstructured network/hybrid, generated using Gambitcommercial code. The network independence test was performed with different number of nodes with special focus on the entrance of the tube, and independence was obtained using 6.5 million cells

(Fig. 3). The full-field grid quality is very good with up to 90% of the cells having a deviation value of 0.45 and no greater than 0.7.

Table 2: Size of the mesh

Arrangement	Grid size
90°	8 887 743
60°	8 852 851
45°	8 846 324
30°	8 932 483

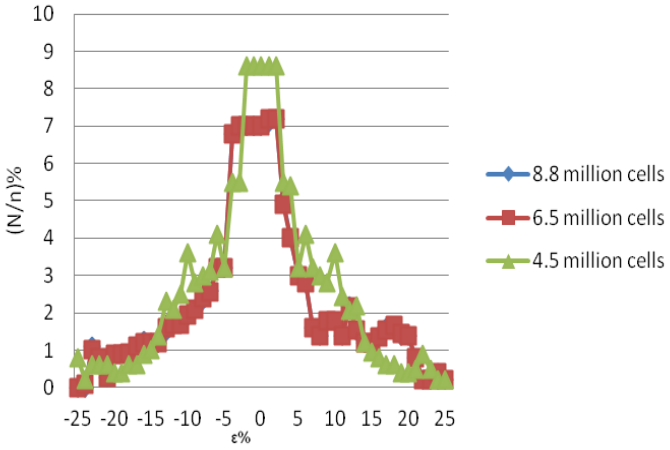

Fig.3. Study of the mesh independence

2.4 Turbulence model

The k-SST model of shear stress transfer is chosen as the turbulence model since this turbulence model significantly improves the accuracy for rapidly strained flows and also has advantages over other turbulence models, for example the k-model, especially for integration through the viscous sublayer and for predicting the detrimental effects of stress gradient [17, 19–21]. For a steady flow, the equations of the form k- SST are as follows:

$$\frac{\partial(\rho u_j k)}{\partial x_j} = P - \beta^* \rho \omega k + \frac{\partial}{\partial x_j}\left[(\mu + \sigma_k \mu_t)\frac{\partial k}{\partial x_j}\right] (4)$$

where is the spatial coordinate, – is the kinetic energy of perturbation, the pressure manifold Pis, β^* is the perturbation model constant SST equal to 0.09, is the specific dissipation rate, – is the molecular dynamic viscosity, σ is the perturbed model constant, u_T is the perturbed viscosity

$$\frac{\partial(\rho\omega)}{\partial x_j} = \frac{\gamma}{v_t} P - \beta \rho \omega^2 + \frac{\partial}{\partial x_j}\left[(\mu + \sigma_\omega \mu_t)\frac{\partial \omega}{\partial x_j}\right] + 2(1 - F_1)\frac{\rho \sigma_{\omega 2}}{\omega}\frac{\partial k}{\partial x_j}\frac{\partial \omega}{\partial x_j} (5)$$

where:

$$P = \tau_{ij}\frac{\partial u_i}{\partial x_j} (6)$$

$$\tau_{ij} = \mu_T\left(2S_{ij} - \frac{2}{3}\frac{\partial u_k}{\partial x_k}\delta_{ij}\right) - \frac{2}{3}\rho k \delta_{ij} (7)$$

$$S_{ij} = \frac{1}{2}\left(\frac{\partial u_i}{\partial x_j} + \frac{\partial u_j}{\partial x_i}\right) (8)$$

$$\mu_t = \frac{\rho a_1 k}{\max(a_1 \omega, \Omega F_2)} (9)$$

$$\emptyset = F_1 \emptyset_1 + (1 - F_1)\emptyset_2 (10)$$

$$F_1 = \tanh(arg_1^4) (11)$$

$$arg_1 = min\left[\max\left(\frac{\sqrt{k}}{\beta^* \omega d}, \frac{500v}{d^2 \omega}\right), \frac{4\rho \sigma_{\omega 2} k}{CD_{k\omega} d^2}\right] (12)$$

$$CD_{k\omega} = max\left(2\rho\sigma_{\omega^2}\frac{1}{\omega}\frac{\partial k}{\partial x_j}\frac{\partial \omega}{\partial x_j}, 10^{-20}\right)(13)$$

$$F_2 = \tanh\left(arg_2^2\right)(14)$$

$$arg_2 = \max\left(2\frac{\sqrt{k}}{\beta^*\omega d}, \frac{500v}{d^2\omega}\right)(15)$$

$$\Omega = \sqrt{2W_{ij}W_{ij}}(16)$$

$$W_{ij} = \frac{1}{2}\left(\frac{\partial u_i}{\partial x_j} - \frac{\partial u_j}{\partial x_i}\right)(17)$$

where - identity matrix or Kronecker delta function, is the magnitude of the eddy

The constants used for the two models, the far field and limit conditions are summarized in Table 3.

Table 3: Constants used in the resolution and limit conditions [20]

Designation	Constants / conditions	values
*k-ω*model	σ_{k1}, $\sigma_{\omega 1}$, β_1	0.50, 0.650, 0.0750
*k-ε*model	σ_{k2}, $\sigma_{\omega 2}$, β_2	1.00, 0.856, 0.0828
SST model	β^*, a_1	0.09, 0.31
Far-field conditions	$\frac{U_\infty}{L} < \omega_{farfield} < 10\frac{U_\infty}{L}$ $\frac{10^{-5}U_\infty^2}{Re_L} < k_{farfield} < 10\frac{0.1U_\infty^2}{Re_L}$	
Limits conditions / wall	ω_{wall} k_{wall}	$= 10\frac{6v}{\beta_1(\Delta d_1)^2}(18)$ $= 0$

2.5 Boundary conditions

In this study, we worked with crude oil at 30° API with physical properties specified at 150°C and 1 atm pressure, υ = 4.016 * 10-6 m2/s and ρ = 783,218 kg/m3 [17, 22]. The condition of the inlet velocity of the inlet of the exchanger head is assigned a value of 1.252 m / s. The speed is uniform and normal to the input surface.

The flow state of the head output is modeled using the outflow state.

The disturbance intensity (0.16〖Re〗^ ((- 1)/8)) and the length scale (0.07Dn) are selected as inputs to the disturbance [21], where Re is the Reynolds number, D_n is the nominal diameter

2.6 Method of resolution

Calculations are performed using Fluent 15.0, a commercial account software. The simple algorithm was chosen to correlate pressure and velocity. For dissociation diagrams, we used:

- Rapid perturbation kinetic energy and specific dissipation rate.

Presto for pressure.

- Momentum of the second order.

-Least squares cell based gradient.

Wind power is second.

For the affinity criteria for each control size, residuals with a value less than 10–5 are superimposed. Computation time is provided for approximately 36 hours on a mobile workstation with Intel i-7-3740 QM CPU, 2.70 GHz.

2.7 Validation of the CFD

To validate the calculation procedure, the numerical results for the 90° case are compared with those obtained using the analytical work found in [17], by calculating the fluid velocity deflection i. The fluid velocity deviation can be calculated by:

$$\varepsilon_i = \frac{U_i - U_m}{U_m} (19)$$

where ε_i is the skew velocity, U_i the velocity at pipe i, and U_m is the mean velocity.

The misdistribution curves, shown in Fig. 3, are based on the velocity deviation for the time interval (ε, ε + Δε). Indeed, the number of tubes may vary in the interval [- | ε | , - | ε | + Δε) for the number in the range [+ | ε | - Δε, + | e |). However, the mathematical model of Muhammad and Al-Malayri [17] is based on a symmetric distribution that takes into account the number of tubes in the intervals [- | ε | , - | ε | + Δε) and [+ | ε | - Δε, + | ε|) are equal. Therefore, a better comparison between the mathematical model and the CFD results will be obtained when the CFD results are presented as an average value, when the arithmetic mean of the digital tubes is then in the ranges [- | ε | , - | ε | + Δε) and [+ | ε | -Δε, + | ε|) the number of tubes in the range [-| ε | , - | ε | + Δε) and the number of tubes in the range [+ | ε | -Δε, + | e |):

$$N_{[-|\varepsilon|,-|\varepsilon|+\Delta\varepsilon)} = N_{[+|\varepsilon|-\Delta\varepsilon,+|\varepsilon|)} = \frac{N_{[+|\varepsilon|-\Delta\varepsilon,+|\varepsilon|)} + N_{[+|\varepsilon|-\Delta\varepsilon,+|\varepsilon|)}}{2} (20)$$

WhereN is the maximum number of tubes with a given velocity deviation interval (_-^+)ε¯.

As such, the obtained curve lies below the mathematical model result curve of Mohammadi and Malayri (2013). These results are satisfactory. Moreover, the maximum velocity deviation | ε | about 25% (Fig. 4).

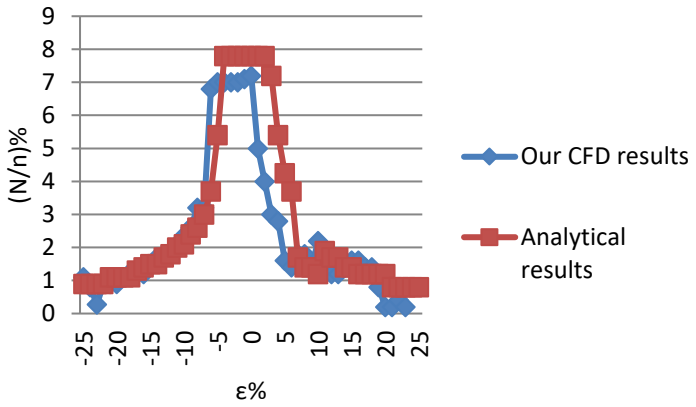

Fig. 4.CFDValidation

3. Results and Discussion

The current study uses CFD tools to simulate the flow behavior in a shell-and-tube heat exchanger. The considered exchanger is a medium-sized industrial one, which has only one lane with a total number of 464 tubes in a 90-degree arrangement [17]. For other arrangements the same parameters are used unless the number of tubes and their pitch.

CFD results in this section are in the average time, due to the attractiveness of turbulent flow.

3.1 Velocity distribution

Figures 5 to 8 display the velocity profiles on the inlet pipe side for all studied arrangements, and the best results were obtained for the 45° arrangement (Fig. 7), where the highest average velocity of 1.25 m/s was recorded, which is similar to the velocity at the inlet. The second best result was obtained for a 90° order

(Fig. 5) with an average velocity of 1.19 m/s, followed by a 60° order (Fig. 6) with an average velocity of 1.167 m/s and finally a 30° order (Fig. 8) with an average velocity of 1.096 m/s.

Noting that the 45-degree arrangement has the highest average speed and the 30-degree arrangement has the lowest, due to the configuration having the fewest and highest number of tubes that can reduce or increase tube resistance.

In addition, the difference between lateral and transverse pitch directly affects the velocity distribution.

The highest and lowest velocity are recorded in the 60° range (Fig. 6) with values of 1.627 m/s and 0.697 m/s, respectively.

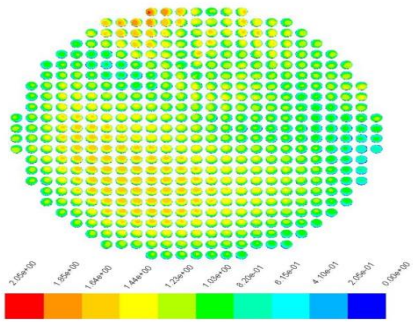

Fig.5. Contour of velocity magnitude for 90° arrangement (m/s)

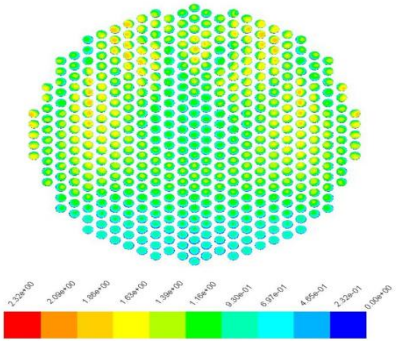

Fig.6. Contour of velocity magnitude for 60° arrangement (m/s)

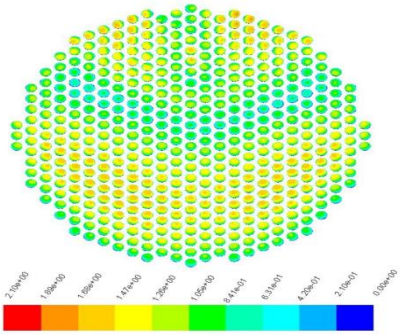

Fig.7. Contour of velocity magnitude for 45° arrangement (m/s)

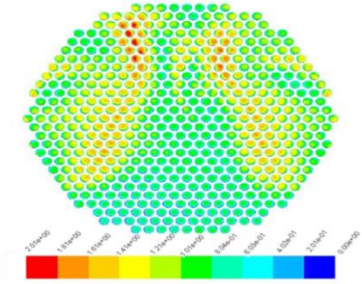

Fig.8. Contour of velocity magnitude for 30° arrangement (m/s)

3.2 Study of theflow distribution uniformity

It is well known that obtaining a perfect flux distribution, in any practical application, is rather impossible. As such, any variation of less than ± 5% in average velocity will be ignored, and the corresponding flow distribution will be considered ideal [16, 17, 23]. The results for the uniformity of the distribution are shown as the proportion of the tube count that has a velocity deviation (Eq. 19) less than 5%, in absolute terms, in reference to the total tube count (Fig. 9-12). Uniformity of distribution curves can be important in the design of tube heat exchangers, as they will provide information on the minimum total number of tubes through which an acceptable flow distribution can be achieved. The flow distribution is:

- larger on the right of the value of ε = 0, with a small tube having minimal flow, in the 60° and 30° arrangements;
- light symmetrical in the case of arrangement at an angle of 90 °;
- higher in the left side of the value = 0, but the dominant part has a smaller deflection, which guarantees a minimum flow if arranged at an angle of 45 degrees.

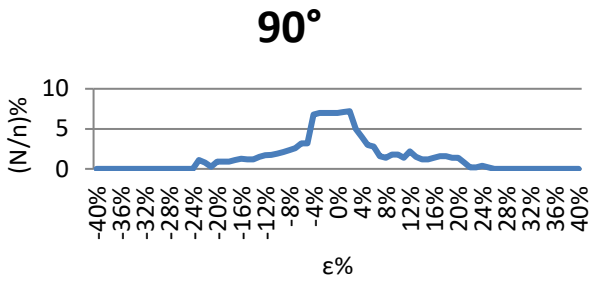

Fig.9. Flow distribution curve for the arrangement of 90°

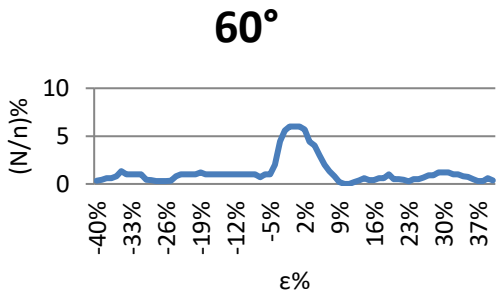

Fig.10. Flow distribution curve for the arrangement of 60°

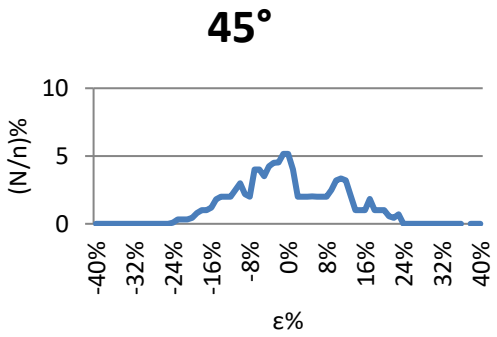

Fig.11. Flow distribution curve for the arrangement of 45°

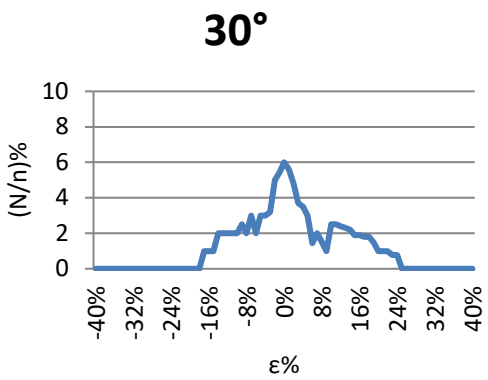

Fig.12. Flow distribution curve for the arrangement of 30°

As mentioned earlier, the misdistribution in a disordered system is not a function of the Reynolds number. However, the velocity deviation depends on the geometrical arrangement of the heat exchanger and may also depend on the Reynolds number. Thus, the ill distribution is not a function of the Reynolds number, but must take into account the effect of geometric aspects of heat exchange around the maximum velocity deviation. Results show that the 60° arrangement is most likely to give better uniformity of flow distribution, with over 46% of pipes with a slight deviation | ε | ≤5%, indicating a high rate tube with uniform distribution. It is followed by an order of 30° then 90° and finally 45°, Fig. 13. It should also be noted that for the 45° range more than 33% of the pipes have a flow rate with a velocity deviation of a value greater than 5%. We find in second place those of the 30° arrangement with more than 29% of the tubes having a deflection in air greater than 5%, then there is the 90° arrangement with approximately 24% with a deflection greater than 5% and in the last position, the 60° arrangement with more than 24% of the tube, Fig. 14.

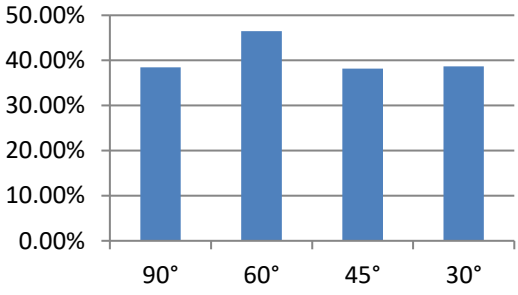

Fig.13. Representation of flow distribution uniformity with | ε | ≤ 5%

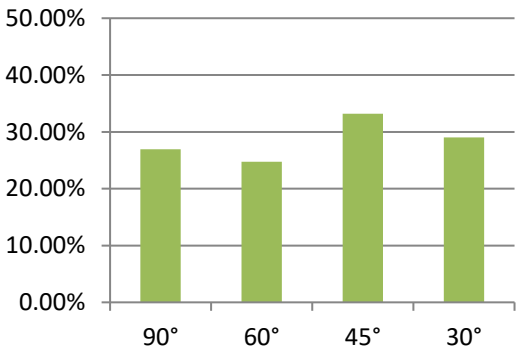

Fig.14. Representation of flow distribution with ε> 5%

4. Conclusion

This work is part of a study of the working performance of a shell and tube heat exchanger. It was of interest to study the flux flow distribution on the heat exchange head because it directly affects the performance and efficiency of the heat exchange. Limited work has been recorded in the area of flow distribution on top of the shell and tube heat exchanger. The aim was to find out whether the tube arrangement affects the flow distribution and to determine the best tube arrangement to obtain a uniform flow distribution, which has not been investigated before. The results show that changing the tube arrangement directly affects the flow distribution. The best registered head distribution, based on the assumption that the best uniformity of the flow distribution is obtained when we have a velocity deviation of -varying between interval [-5%, +5%], is the worst order of 60° and the distribution is recorded on the order of 45°. Thus, 71.36% of the total pipe is recorded for the last arrangement (45°), which has a more variable velocity deflection [-5, +18] with the largest average velocity equal to the initial flow velocity, while for the 60° value arrangement, 71.22% deflection [-5, 40] is recorded with an average velocity less than the value exchange rate of approx.

Therefore, the arrangement which represents the best uniformity of flow distribution is 60° but has a large number of tubes also with a low flow velocity. The arrangement that guarantees a higher speed with the maximum number of tubes having almost unchanged speed is 45°.

References

[1] Mueller A. Effects of some types of maldistribution on the performance of heat exchangers. Heat transfer engineering 1987;8:75-86.

[2] Venkatesan Y. Effect of maldistribution and flow rotation on the shell side heat transfer in a shell and tube heat exchanger: Wichita State University; 2011.

[3] Acrivos A, Babcock B, Pigford R. Flow distributions in manifolds. Chemical Engineering Science 1959;10:112-24.

[4] Kubo T, Ueda T. On the characteristics of divided flow and confluent flow in headers. Bulletin of JSME 1969;12:802-9.

[5] Mohan G, Rao BP, Das SK, Pandiyan S, Rajalakshmi N, Dhathathreyan K. Analysis of Flow Maldistribution of Fuel and Oxidant in a PEMFC. Journal of energy resources technology 2004;126:262-70.

[6] Saber M, Commenge J-M, Falk L. Rapid design of channel multi-scale networks with minimum flow maldistribution. Chemical engineering and processing: process intensification 2009;48:723-33.

[7] Rebrov EV, Schouten JC, De Croon MH. Single-phase fluid flow distribution and heat transfer in microstructured reactors. Chemical Engineering Science 2011;66:1374-93.

[8] Gandhi MS, Ganguli AA, Joshi JB, Vijayan PK. CFD simulation for steam distribution in header and tube assemblies. Chemical Engineering Research and Design 2012;90:487-506.

[9] Wang J, Gao Z, Gan G, Wu D. Analytical solution of flow coefficients for a uniformly distributed porous channel. Chemical engineering journal 2001;84:1-6.

[10] Wang J. Pressure drop and flow distribution in parallel-channel configurations of fuel cells: Z-type arrangement. International journal of hydrogen energy 2010;35:5498-509.

[11] Wang J. Theory of flow distribution in manifolds. Chemical engineering journal 2011;168:1331-45.

[12] Fang L, LUO Y-h, YANG S-m. Analytical and experimental investigation of flow distribution in manifolds for heat exchangers*. Journal of Hydrodynamics, Ser B 2008;20:179-85.

[13] Bhutta MMA, Hayat N, Bashir MH, Khan AR, Ahmad KN, Khan S. CFD applications in various heat exchangers design: A review. Applied Thermal Engineering 2012;32:1-12.
[14] Habchi C, Lemenand T, Della Valle D, Peerhossaini H. Turbulent mixing and residence time distribution in novel multifunctional heat exchangers–reactors. Chemical engineering and processing: process intensification 2010;49:1066-75.
[15] Putnam GR, Rohsenow WM. Viscosity induced non-uniform flow in laminar flow heat exchangers. International journal of heat and mass transfer 1985;28:1031-8.
[16] Hewitt GF, Barbosa J. Heat exchanger design handbook: Begell House; 2008.
[17] Mohammadi K, Malayeri M. Parametric study of gross flow maldistribution in a single-pass shell and tube heat exchanger in turbulent regime. International Journal of Heat and Fluid Flow 2013;44:14-27.
[18] Kuppan T. Heat exchanger design handbook: CRC; 2000.
[19] Wilcox DC. Turbulence modeling for CFD: DCW industries La Canada, CA; 1998.
[20] Menter FR. Two-equation eddy-viscosity turbulence models for engineering applications. AIAA journal 1994;32:1598-605.
[21] Guide FUs. Version 15, ANSYS. Inc, April 2014.
[22] Jones DS, Pujadó PP. Handbook of petroleum processing: Springer Science & Business Media; 2006.
[23] Shah RK, Sekulic DP. Fundamentals of heat exchanger design: John Wiley & Sons; 2003.